Field measurements of airborne concentration and deposition rate of maize pollen

Nathalie Jarosz, Benjamin Loubet, Brigitte Durand, Alastair Mccartney, Xaxier Foueillassar, Laurent Huber

FIELD MEASUREMENTS OF AIRBORNE CONCENTRATION AND DEPOSITION RATE OF MAIZE POLLEN

Nathalie Jarosz[1], Benjamin Loubet[1], Brigitte Durand[1], Alastair McCartney[2], Xavier Foueillassar[3] and Laurent Huber[1]

[1] *National Institute of Agronomic Research (INRA), UMR-EGC, 78850 Thiverval-Grignon, France*
[2] *Rothamsted Research, Harpenden, Hert, AL5 2JQ, UK*
[3] *AGPM technique, 21 Chemin de Pau, 64121 Montardon, France*

Agricultural and Forest Meteorology, 119 (2003), 37-51

ABSTRACT. In recent years there has been interest in the dispersal of maize (*Zea mays*) pollen from crops, particularly in relation to gene flow and seed quality. We report the results of experiments that measured maize pollen dispersal from a 20 m × 20 m experimental crop. The experiments were done in a commercial farm in France during the summer of 2000. Pollen production was estimated to range from 10^4 to 2×10^6 grains per day per plant. Pollen concentrations and deposition rates decreased rapidly with distance from the crop: concentrations decreased by about a factor of 3 between 3 m and 10 m downwind of the source; deposition rates at 30 m were less than 10% of those at 1 m. Horizontal flux of pollen were estimated from pollen concentration and wind speed profiles using a mass balance approach, and ranged from 5 to 560 grains m^{-1} s^{-1} at 3 m from the source. Comparison of deposition rates estimated with the mass balance and direct measurement suggests that only a small proportion of the pollen released from the crop would have been still airborne at distances greater than 30 m downwind. Deposition velocity determined as the ratio of the deposition rate to the airborne concentration at 3 m from the source averaged 0.6 m s^{-1}, which is twice as large as the settling velocity for maize pollen.

KEYWORDS: Maize, pollen, particle dispersion, concentration profile, deposition velocity, aerobiology

1 INTRODUCTION

Over the last few years there has been an increasing interest in pollen dispersal, particularly in relation to gene flow from transgenic crops (Lavigne *et al.*, 1998; Klein, 2000) and the maintenance of seed quality. Maize (*Zea mays*) is primarily wind pollinated and is one of the most cultivated cereal crop in many parts of the world. Transgenic maize cultivars are widely grown in North America. However, at present there are concerns about possible gene transfer from transgenic maize crops to non-transgenic crops.

There have been surprisingly few studies reporting pollen dispersal from maize crops. The studies of Raynor *et al.* (1970, 1972a, 1972b) are probably the most comprehensive. They measured atmospheric concentrations and deposition rates of maize pollen at different

distances downwind of two circular experimental plots of 18.3 m diameter. They noted that concentration and deposition of maize pollen were several times smaller than those for timothy (*Phleum pratense*), a grass, and ragweed (*Ambrosia artemisiifolia*), an anemophilous weed. Maize pollen grains are roughly spherical with diameters around 90 µm (Di-Giovanni *et al.*, 1995) and are much larger than either timothy (about 40 µm) or ragweed (18 – 20 µm) pollen. Raynor *et al.* (1970, 1972a, 1972b) clearly showed a quantitative effect of the grain size on dispersion and deposition of pollen. The other outcome of their studies was to determine the isolation distance required for production of purebred seed. They found that concentration and deposition of maize pollen declined rapidly with distance from the plot. However, the meteorological conditions during their experiments were not reported in sufficient detail to enable validating a dispersion model for maize pollen. Without the use of such model, it would be hard to draw generalised conclusions about distance of maize pollen dispersal in a range of climatic conditions.

In this study, we present the results of an experiment where vertical and horizontal profiles of airborne maize pollen concentrations and deposition rates were measured downwind of a 20 × 20 m maize plot. We also present estimates of horizontal fluxes of maize pollen at two distances downwind from the source and discuss their validity.

2 MATERIAL AND METHODS

2.1 Experimental site

The experiment were done between the 24 July and the 6 August 2000, on a commercial farm at Montargis (lat. = 48°00′N; long. = 2°44′E; alt. = 90 m), France. The experimental design consisted of a 20 × 20 m plot of maize, thereafter called source plot, cultivar Adonis (blue grains Pau Semences, France), located in the centre of a 120 × 122 m area of bare soil (Figure 1). The plot and surrounding bare soil was located in the middle of a 184 × 240 m maize field (target field), cultivar Adonis. The maize in the plot and surround was sown on 17 May at a sowing density of 98,000 plants ha^{-1}. The experimental site had woodland (approximately 15 m tall) to the north, east and west. Two farm buildings were also to the

north (Figure 1). Measurements were made of the dispersal of maize pollen downwind of the central source plot on 12 occasions during flowering. The experiments are referred to as R1 to R12 in the rest of the paper. The downwind distance from the source will be called hereafter *x*, and the height above the ground *z*. All times are given in universal time, UT (≡ GMT), which is the local time minus 2h during the experiment, and was very close to the solar time. This experiment was conducted in parallel with an other experiment to measure cross-pollination of the target field by the source plot. **(INSERT FIGURE 1)**

The heights of the highest leaf (canopy height), the tassel and the ear were measured on 30 plants in the source plot on 31 July. The median height of the base and the top of the tassels were 2.2 and 2.5 m (± 10%, standard deviation/median) respectively, the median canopy height was 2.28 m (± 9%), and the median height of the ears was 1.1 m (± 8%).

2.2 Micrometeorological measurements

Wind speed, wind direction, air temperature, relative humidity, surface wetness index and global radiation were measured in the centre of the source plot. The instruments were mounted on several masts. The name, type and height of each instrument are given in Table 1. Net radiation, soil heat flux and rain were measured in the bare soil area. Measurements were recorded every 5 seconds using a Campbell CR10 datalogger (Campbell Scientific, UK), and averaged over 15 min. During each experiment a 3D ultrasonic anemometer was operated in the centre of the source plot, another above the bare soil area, and a third above the target field (Figure 1, Table 1). Unfortunately, the sonic anemometer placed above the target field did not work during some of the experiments. The friction velocity (u_*) and the Monin-Obukhov length (L) were therefore estimated as the average of the two other sonic anemometers. The values of u_* and L were very similar for these two sonic anemometers, and were representative of the bare soil surface. Wind speed profiles, up to $z = 4$ m, were measured at $x = 3$ and 10 m downwind from the source plot using cup anemometer (see Table 1 for measurements heights). All meteorological data were averaged over each run to ease the comparison between runs, and to provide input data for future dispersion modelling.

(INSERT TABLE 1)

2.3 Pollen Measurements

Pollen concentration in the source plot. A 7-day recording spore trap (Burkard Manufacturing Co., Rickmansworth, U. K.) was placed in the centre of the source plot with its inlet orifice at about the height of the tassels, and was operated continuously throughout the experiment. The operation of this type of trap is described in detail elsewhere (British Aerobiology Federation, 1995; Lacey and Venette, 1995). Briefly, the trap collected spores on a clear film (Melinex tape, Burkard Manufacturing Co., Rickmansworth, UK) attached to a slowly rotating drum, allowing pollen concentration to be recorded over a 7 day period. The tape surface was coated with a mixture of petroleum jelly and paraffin wax (British Aerobiology Federation, 1995). After exposure, each tape was cut into 48 mm sections, representing 24 hours exposure periods, and was permanently mounted on a microscope slide using Gelvatol (Burkard Manufacturing Co., Rickmansworth, UK) and a glass coverslip (British Aerobiology Federation, 1995). The hourly concentrations of maize pollen grains were estimated by counting them on 2mm wide transects using a light microscope.

Pollen production. The pollen production per plant per day was determined using the same 5 individual plants each day. Polythene bags Osmolux (Pantek, France) were placed over the whole tassel at 09:00 UT every day and left for a period of 24 hours. The pollen grains that accumulated in the bags were collected in bottles containing electrolyte solution (Coulter Isoton, Beckman, USA). The number of pollen grains collected was estimated by counting sub-samples with a cell counter (Coulter Multisizer III, Beckman, USA). The proportion of flowering plants in the field was also estimated by observing the number of plant that has started flowering and the number of plants that had finished flowering for 25 plants in the plot each day. These observations and the measurements of pollen production from the marked plants were used to estimate the daily pollen production in the whole plot. The production during each run was estimated by multiplying the daily production by the ratio of pollen

concentration in the crop integrated over the run to pollen concentration integrated over the whole day.

Pollen concentration downwind of the source plot. Vertical profiles of pollen concentration were measured at x = 3 and 10 m downwind of the source plot using 4 m tall "mass balance" masts (the same masts used for wind speed profiles). Pollen concentrations were measured at 5 heights (0.25, 0.5, 1.0, 2.0 and 4.0 m above the ground) using rotating-arm spore traps (McCartney and Lacey, 1991; McCartney *et al.*, 1997). The traps were built at INRA based on the design of McCartney and Lacey (1991), with slight changes. Each trap was made from a 2 mm square section brass rod bent into a U-shape to give two vertical arms, 50 mm long and 78 mm apart (diameter of the trap, d_a). The arms were attached to 12V electric motors that rotated between 3000 and 4000 rpm, depending on the applied voltage (equivalent air sampling rate of 158 and 210 l min^{-1}). The rotational velocity (ω) of each trap was calibrated against applied voltage, which was measured before and after each experiment to estimate the rotation speed of each individual trap. Pollen grains were collected on two acetate strips (approximately 2.15 mm wide (l) and 50 mm high (h)) glued to the leading edge of the vertical arms. The strips were covered with a thin layer of silicon grease to retain the catch. After each run, these slides were detached and permanently mounted on a microscope slide as for the Burkard samples, prior to visual counting using a light microscope. The airborne pollen concentration, C, was determined assuming an impaction efficiency of 0.86 (Aylor, 1982), according to the following equation:

$$C = \frac{N}{0.86\ \pi\, d_a\ \omega\, l\, h\ \Delta t} \qquad (1)$$

where N is the average number of pollen grains per arm for each trap, d_a is the rotating-arm diameter, ω is the rotational velocity, l is the width of the rotating-arm, h is its height, and Δt is the duration of each run. The masts were moved before each experiment so that they were aligned within the downwind fetch of the source. The rotating-arm traps were operated for periods of between 90 and 180 min.

The horizontal flux of pollen at height z, $F_x(z)$, was estimated from the mean averaged pollen concentration, $C(z)$ and wind speed, $U(z)$ as $F_x(z) = C(z).U(z)$, neglecting the turbulent component of the horizontal flux $\overline{u'c'}$, where u' and c' are the fluctuating component of the wind speed and concentration, respectively (see discussion section for an estimation of this term). The integrated horizontal flux passing through each mast, $F_{\mathbf{x}}^{\{0\text{-}4\}}$, was estimated by integrating $F_x(z)$ from z = 0 to 4 m using the trapezoidal method. Since the $F_x(z)$ should be zero at the lower boundary, due to a zero wind speed, the measured $F_x(z)$ was extrapolated to $F_x(0) = 0$. The roughness length z_0 and the displacement height d were neglected, as they are small over a bare soil.

Pollen deposition to the ground. The deposition rate of pollen was estimated using small containers (diameter = 50 mm, height = 70 mm), containing approximately 30 ml of Coulter Isoton. The containers were placed 1, 2, 3, 4, 8, 10, 16 and 32 m downwind of the source plot along three lines. The tops of the containers were at 0.35 m above the ground for one line and at 0.15 m for the two others. They were opened at the beginning of each run and closed at the end. The number of pollen grains collected in each container was estimated by first filtrating the sample, rinsing the filters with Coulter Isoton, taking four 100 µl sub-samples, and counting the number of pollen grains in each sample using a binocular microscope. Deposition rates were calculated from estimates of the number of pollen grains collected and time of exposure. The deposit traps were operated for the same time as the rotating-arm traps (see Table 2). The integrated deposition rates between x = 1 and 3 m ($D_{1\text{-}3}$), x = 3 and 10 m ($D_{3\text{-}10}$), and x = 1 and 32 m ($D_{1\text{-}32}$), were estimated by integrating the measured deposition along x, using a trapezoidal rule. As this integration is one dimensional, the integrated deposition rate is not the total deposition as a function of distance. The deposit between x = 3 and 10 m was also estimated, using the mass balance method, as the difference between the integrated horizontal fluxes measured with the masts at these distances ($\Delta F_{3\text{-}10}$):

$$\Delta F_{3\text{-}10} = F_3^{\{0\text{-}4\}} - F_{10}^{\{0\text{-}4\}} \qquad (2)$$

Equation (2) assumes that three components of the mass balance can be neglected: (i) the turbulent component of the horizontal flux ($\overline{u'c'}$) at each distance, (ii) the vertical flux

through the lid of the volume delimited by the two masts ($F_z(z = 4\ m)$), and (iii) the divergence of the lateral flux ($\partial F_y / \partial y$). The validity of these assumptions is evaluated in the discussion section.

3 RESULTS

3.1 Micrometeorological measurements

The spring and early summer of 2000 at Montargis were particularly wet, which delayed the growth and flowering of the maize crop. During the experimental period, rain occurred on the first 4 days, however it only rained during run R8, and run R3 was interrupted due to rain. Average values of micrometeorological variables for each run are given in Table 2. During most runs, wind speed was low, mean solar radiation ranged between about 100 W m^{-2} and 750 W m^{-2}, and relative humidity varied from 50% to 83%. During all runs the thermal stratification of the surface boundary layer was unstable, as shown by the negative Monin and Obukhov length and the large standard deviations for wind direction (5° to 52°). During run R9, the air flow was probably close to free convection. For 8 of the runs the mean wind direction relative to the direction of the masts and containers was less than 20°; for three of them it was between 30° and 40° (R3, R10 and R12), and for run R9, it was greater than 100°. **(INSERT TABLE 2)**

3.2 Pollen production

Pollen production began on 26 July and lasted 14 days, with the maximum production occurring on the 1-2 August (Table 3). The number of pollen grains emitted per day per plant ranged from 10^4 to 2×10^6, which corresponds to roughly 5×10^7 to 7×10^9 grains day^{-1} for the whole source plot. Over the pollination period, pollen production was on average 1.4×10^7 grains $plant^{-1}$. **(INSERT TABLE 3)**

3.3 Pollen concentration in the source plot

Figure 2 shows the 2-hourly moving average pollen concentration measured above the source plot between the 24 July and 3 August. The concentration had a clear diurnal periodicity and the daily maximum had a similar dynamics as the estimated pollen production over the period (Figure 2). **(INSERT FIGURE 2)**

The daily pattern of pollen concentration between 29 July and 3 August, is shown in Figure 3a, together with the surface wetness index (*SWI*), as measured by the wetness sensors. *SWI* tended to fall from nearly 100% (wet) to nearly 0% (dry) as pollen started to be released, except for the 3 August (Figure 3a). The daily pattern, normalised by the daily maximum concentration, and averaged over the five first days of Figure 3a is plotted in Figure 3b. It shows that pollen emission began at about 0800 UT and ended at about 1600 UT, and the maximum concentration occurred at around 1000 UT. Almost no pollen was trapped at night (between 1800 and 0600 UT), although small peaks were occasionally observed. The pattern on 3 August was unusual as the concentration started to increase at around 0600 UT. **(INSERT FIGURE 3)**

3.4 Vertical profiles of pollen concentration

All vertical profiles of pollen concentration had a similar shape, with the maximum concentration always located below 2 m, for profiles at x = 3 m from the source and below 1 m, for profiles at x = 10 m from the source. Profiles for runs R6, R7 and R8 are shown in Figure 4. As expected, the concentration decreased with distance downwind of the source and generally decreased with height above 2 m. Concentrations ranged from 0 to 210 grains m^{-3}, 3 m downwind and from 0 to 45 grains m^{-3}, 10 m downwind. **(INSERT FIGURE 4)**

3.5 Wind speed and horizontal flux of pollen

Figure 5 shows the vertical profiles of wind speed at x = 3 m and 10 m averaged over all runs. In the figure the values of wind speed have been normalised by the speed of the highest anemometer at each mast, which corresponded to the highest wind speed (between 1.1 and

2.4 m s^{-1}). At x = 3 m downwind of the source, the wind speed profile was greatly influenced by the source plot, as showed by the depletion of the profile. At x = 10 m, the wind speed profile is closer to the unperturbed profile (log profile in Figure 5), indicating that the influence of the source plot is getting weaker. A log profile with a roughness length, z_0 = 0.07 m, mimics the measured profile at x = 10 m, which corresponds to a farmland with many hedges according to Panofsky and Dutton (1984). **(INSERT FIGURE 5)**

The vertical profiles of horizontal flux of pollen grains ($F_x(z)$) are shown in Figure 6 for 3 typical runs (R6-R8). Fluxes were greater at x = 3 m than at x = 10 m. The fluxes $F_x(z)$ ranged from 0 to 200 grains m^{-2} s^{-1} and, for the 3m mast, the maximum value usually occurred at about z = 2 m. It is difficult to extrapolate the profile of $F_x(z)$ above z = 4 m, as the slope were not always negative between z = 2 and 4 m, especially at x = 10 m. However, using a linear extrapolation from the two highest points of the profile at x = 3 m, the flux above z = 4 m was found to represent about 40% of $F_3^{\{0\text{-}4\}}$. However, this is probably overestimated since the flux profile at x = 3 m would probably decrease exponentially with height.

(INSERT FIGURE 6)

The integrated horizontal fluxes passing through the masts $F_3^{\{0\text{-}4\}}$ and $F_{10}^{\{0\text{-}4\}}$ are shown in Table 4. The flux at 10 m was usually between ¼ and ½ of that at 3 m. The flux $F_3^{\{0\text{-}4\}}$ ranged from 1 to 560 grains m^{-1} s^{-1}, which is an order of magnitude smaller than the estimated pollen production per m width of the source plot.

3.6 Pollen deposition

Figure 7 shows the measured pollen deposition rates divided by the deposition rate at x = 1 m as a function of the downwind distance from the source. The actual deposition rates can be estimated by multiplying the values in Figure 7 by the deposition rate measured at x = 1 m (Table 4). Deposition rates decreased with distance downwind of the source and ranged from 10 to 150 grains m^{-2} s^{-1} between x = 1 and 10 m, and from 3 to 10 grains m^{-2} s^{-1} between x = 16 and 32 m. The integrated deposition rates between 1 and 3 m, 1 and 32 m and 3 and 10 m downwind from the source ($D_{1\text{-}3}$, $D_{1\text{-}32}$ and $D_{3\text{-}10}$ respectively) are given in Table 4. The

difference between the integrated horizontal fluxes at x = 3 and 10 m, $\Delta F_{3\text{-}10}$ (Eq. 2) generally compared well with $D_{3\text{-}10}$ (Table 4). **(INSERT FIGURE 7) (INSERT TABLE 4)**

4 DISCUSSION

4.1 Dynamics of pollen emission

The pollen concentration in the crop had a marked diurnal periodicity with the maximum concentration usually occurring in the morning at around 1000 UT, a pattern common to wind pollinated plants (Scott, 1970; Gregory, 1973). However, we never found a bimodal pattern of pollen concentration as observed by Flottum *et al.* (1984) for sweet corn pollen. The start of pollen emission in the morning appeared to coincide with the drying of the crop (Figure 3a). This may explain why pollen emission started earlier on 3 August than on previous days (Figure 3b), as the crop remained almost dry during the previous night (as indicated by the small surface wetness index).

4.2 Airborne pollen concentrations

The shapes of the vertical concentration profiles were fairly consistent between runs as indicated by the small error bars in Figure 8, which show the standard deviation of the profiles over all runs. The maximum concentration occurred at about 1 m height at x = 3 m and at about 0.5 m height at x = 10 m, indicating a settling of the pollen plume with distance. An exponential curve ($C(z) = A \exp(-\alpha z)$) was fitted to the average profiles above 1 m height. The coefficient α, which relates to the rate of decrease in concentration with height, was 0.46 m^{-1} and 0.26 m^{-1} at x = 3 m and x = 10 m, respectively, and the regression was quite good (R^2 = 95% and 99% respectively). These values are similar to those found by McCartney and Lacey (1991) for oilseed rape pollen near the edge of the crop. **(INSERT FIGURE 8)**

The pollen concentrations tended to be larger than those reported by Raynor *et al.* (1972a), but this probably only reflects a difference in pollen production by the source. Indeed, although no quantitative estimate of the production is given by Raynor *et al.* (1972a), it was probably smaller as the plant density was 3 to 6 times smaller than in the present study

(15,210 plants ha^{-1} to 37,640 plants ha^{-1}) and they used two or three cultivars with different flowering dates in order to prolong pollination period. However, they also found that sweet corn pollen concentrations decreased rapidly with distance downwind of the source plot. They found that the concentration at 1.5 m above the ground, which corresponded to 1.07 times the height of the tassels, decreased by a factor of roughly two between x = 3 m and 10 m. In this study the concentration decreases by a factor of 3 at the same height relative to the tassels (2.7 m). The larger deposition gradient observed in the present study may be due to a larger turbulence intensity generated by the canopy being taller in this study than in that of Raynor *et al.* (1972a). McCartney and Lacey (1991) found that the pollen concentration at 0.8 m height (just below flower height) downwind of a $20\ m \times 20\ m$ spring oilseed rape plot decreased by a factor of 3.7 on average between x = 3 m and x = 10 m, which is even larger than in this study. Oilseed rape pollen has a much smaller settling velocity ($0.017\ m\ s^{-1}$) than maize pollen, thus we would expect that the horizontal concentration gradient would be shallower as deposition rates would be less. However, the lighter oilseed rape pollen grains may have been more rapidly dispersed vertically and in the crosswind direction, which would have made the concentration gradients steeper.

4.3 Validity of the integrated deposition and mass balance approaches

The integrated deposition rates were estimated by one-dimensional integration over x. However, as shown by Raynor *et al.* (1972a) the pollen dispersion is clearly three-dimensional. The total deposition rate could be estimated by multiplying the integrated deposition rate by a Gaussian function expressing the diffusion of pollen as a function of distance in the cross-wind direction provided that the mean wind direction relative to the direction of the masts is correct.

The horizontal flux difference $\Delta F_{3\text{-}10}$, was well correlated with the integrated deposition rate $D_{3\text{-}10}$ (Figure 9). **(INSERT FIGURE 9)**

This means that the other components of the mass balance (turbulent component of the flux $\overline{u'c'}$, vertical flux at z = 4 m $F_z(z = 4\ m)$, and divergence of the lateral flux $\partial F_y / \partial y$)

between the two masts either are small or cancel each other. Their magnitude and direction are discussed here:

- For gaseous compounds under homogeneous conditions, the turbulent component of the horizontal flux ($\overline{u'c'}$) is generally negative downwind of a source, and of the order of 10% to 20% (Wilson and Shum, 1992; Denmead *et al.*, 1998). However, due to inertia and "crossing-trajectories" effects (Snyder and Lumley, 1971;Reynolds, 2000), $\overline{u'c'}$ for heavy particles, such as maize pollen, should be smaller. Nevertheless, turbulence intensity increases immediately downwind of a roughness change (Gash, 1986), or a windbreak (Heisler and DeWalle, 1988), up to 3 times its magnitude in normal conditions at distances several times the height of the canopy. Coherent structures are also present downwind of such obstacles (e.g., Zhuang and Wilson, 1993). These two effects are likely to increase the magnitude of $\overline{u'c'}$ at x = 3 m and 10 m, downwind of such a small source plot (20 m × 20 m), behaving roughly like a windbreak. Moreover, the large gradients in horizontal turbulent kinetic energy near the downwind edge of the field are likely to induce turbophoretic fluxes, which is a convective drift down gradient of velocity variance (Reynolds, 2000; Wilson, 2000). In addition to these effects, the fact that the maize pollen might be liberated in gusts of wind may bring a positive contribution to $\overline{u'c'}$, since in such a case, u' is positive (by definition of a gust), when c' is positive (pollen is present). This later contribution might diminish or balance the negative contribution due to the increase in turbulence kinetic energy.
- The vertical flux through the lid of the control volume at z = 4 m can be seen as the sum of a “convective flux”, due to the average vertical component of the wind speed ($\overline{w}$), which is non zero downwind of a roughness change, a “settling flux” due to the settling speed of the pollen, a “diffusive flux”, which includes “diffusion” due to gradient in pollen concentration, and a “turbophoretic flux” due to gradient in turbulence intensity and turbulence length scale. The concentration gradient “diffusive flux” should be positive as it stands above the height of the source. In contrast, the “convective flux” should be negative as the average vertical wind speed is directed towards the ground. Similarly, the

"settling flux" is negative. The "turbophoretic flux" may be positive as the vertical gradient of turbulent kinetic energy is negative above the height of the canopy at small distances downwind of the obstacle (The turbophoretic flux is opposed to the gradient of particle velocity variance, Reynolds, 2000). Although we can draw some qualitative analysis, we do not have sufficient measurements to determine the sign and the magnitude of $F_z(z = 4\ \text{m})$.

- Divergence of the lateral flux ($\partial F_y / \partial y$) is certainly non-zero, however, to our knowledge, there are no reported measurements to estimate its contribution. All we can ascertain is that, as shown by Raynor *et al.* (1972a) inertia effects would diminish lateral diffusion of maize pollen compared to smaller pollens (ragweed and timothy) and gases.

In addition, to these potential errors, when the wind angle to the mass balance masts increased in magnitude, several errors might appear: (i) the two mast might not see the same part of the source, (ii) the effective distance of the two mast to the source increases, and (iii) when the wind angle is greater than 45°, the mast at $x = 10$ m might stand outside the fetch of the source. For these reasons the comparison between $D_{1\text{-}3}$ and $\Delta F_{3\text{-}10}$ in Figure 9 has different symbols when the wind angle was larger than 30 degrees.

The different terms of the mass balance discussed here above need more work to be quantified. They could probably be estimated with the use of a Lagrangian stochastic model such as described by Aylor and Flesch (2001), or Reynolds (2000), which could be extended to 3D turbulence, despite the uniqueness problem (Thomson, 1987; Leuzzi and Monti, 1998).

4.4 Deposition and horizontal fluxes of pollen

The shape of the deposition gradient downwind of the source was fairly consistent for most of the experimental runs (Figure 7), with deposition rate decreasing rapidly with distance from the source. On average the deposition rates at distances greater than 20 m were less than 20% of the rate at 1 m, and less than 10% at 32 m. However, the deposition gradients found here were shallower than those found by Raynor *et al.* (1972a), where deposition rates 10 m and 20 m downwind were 6% and 1% of those 1 m from the source, respectively. On

several occasions the maximum deposition rate was observed at larger distances than x = 1 m (Figure 7). On those occasions, u_* was larger than during the other runs, suggesting more effective horizontal transport of pollen grains. Deposition rates tented to slightly increase between x = 16 and 32 m probably because of the presence of the target field at x = 50 m.

It is difficult to accurately estimate the flux of pollen leaving the plot as the closest measurements were made 3 m from the edge. However, a rough estimate can be made by adding the integrated deposition rate from x = 1 to 3 m, in a metre wide strip, to the flux estimated at the two masts (Table 4), neglecting the horizontal flux passing above z = 4 m and the turbulent component of the flux. It appears that about 60% of the pollen released at the edge of the plot was still airborne 3 m downwind and about 30% at 10 m. Differences between $F_3^{\{0\text{-}4\}}$ and $F_{10}^{\{0\text{-}4\}}$ were generally accounted for by deposition, suggesting that pollen above 4 m effectively remained airborne at x = 10 m. The estimates of $F_3^{\{0\text{-}4\}}$ are nearly always less than $D_{3\text{-}32}$ and $D_{3\text{-}16}$. This discrepancy suggests that a large fraction of the horizontal flux is passing over z = 4 m at x = 3 m. As discussed in the previous section, it is difficult to know whether $\overline{u'c'}$ is positive or negative at x = 3 m. These results emphasised the need to measure concentration higher than 4 m.

4.5 Deposition velocities

Maize pollen deposition velocities (V_d = deposition rate / concentration) were estimated at x = 3 and 10 m using concentrations measured 0.25 m above the ground. Values ranged between 0.2 m s^{-1} and 1.8 m s^{-1} and averaged 0.6 ± 0.1 m s^{-1} and 0.7 ± 0.5 m s^{-1} at x = 3 and 10 m, respectively. (Raynor *et al.*, 1972a) found similar values: 0.3 m s^{-1} to 0.8 m s^{-1} for concentrations measured at 0.5 m height and distances of 7.7, 15.3 and 32 m downwind; and 0.6 m s^{-1} to 1.9 m s^{-1} for concentrations measured at 1.5 m height and 9.2, 15.3 and 32 m downwind. Values of V_d were roughly between 2 and 3 times the settling velocity, V_s, reported for maize pollen (0.2 - 0.3 m s^{-1}, Di-Giovanni *et al.*, 1995). A similar discrepancy between V_s and V_d has been observed by Raynor *et al.* (1972a) downwind of a maize field and by McCartney and Aylor (1987) for *Lycopodium* spores in a wheat canopy. As mentioned in

the previous section, "convective" and "turbophoresis" fluxes should enhance deposition just downwind of the source plot, which explains the observed ratio V_d/V_s. However, V_d was not significantly different between x = 3 m and 10 m, although it was more scattered at 10 m.

5 CONCLUDING REMARKS

The results of this study concur broadly with the few published studies for maize pollen dispersal. It is clear that both pollen concentration and deposition rates decrease rapidly with distance from the edge of the source. Although large number of maize pollen grains are produced by a maize crop these experiments suggest that only a relatively small proportion may escape from the maize crop. Our estimates of the flux of pollen escaping from the plot, combined with deposition measurements, suggest most of the pollen released was deposited within about 30 m of the plot. Indeed, roughly 95% of pollen emitted is deposited at 10 m from the source and 99% at 30 m.

The work presented here was done under relatively low wind speeds, thus further experiments may be needed to determine whether pollen dispersal would be enhanced under windier conditions. The pollen deposition within the source (both ground and foliage), although not being the focus of interest here, should be studied in more detailed, as it represents the largest deposition fraction, and therefore the largest uncertainty on the quantity emitted. It would also give valuable information on the deposition processes to silks. These results, however, will provide useful data for testing and validating pollen dispersal models, which would be useful for studying the role of long distance dispersal in the analysis of gene flow in maize.

ACKNOWLEDGEMENTS

The research program “AIP OGM-Environnement”, INRA (Institut National de la Recherche Agronomique), FNPSMS (Fédération Nationale de la Production des Semences de Maïs et Sorgho) and GNIS (Groupement National Interprofessionel des Semences et plants) supported

this work. Rothamsted Research receives grant-aided support from the Biotechnology and Biological Sciences Research Council of the UK.

REFERENCES

Aylor, D.E., 1982. Modeling spore dispersal in a barley crop. Agricultural Meteorology, 26(3): 215-219.

Aylor, D.E. and Flesch, T.K., 2001. Estimating spore release rates using a lagrangian stochastic simulation model. Journal of Applied Meteorology, 40: 1196-1208.

British Aerobiology Federation, 1995. A guide to trapping and counting. c/o Dr J. Lacey, IACR-Rothamsted, Harpenden, Herts AL5 2JQ, UK.

Denmead, O.T., Harper, L.A., Freney, J.R., Griffith, D.W.T., Leuning, R. and Sharpe, R.R., 1998. A mass balance method for non-intrusive measurements of surface-air trace gas exchange. Atmospheric Environment, 32(21): 3679-3688.

Di-Giovanni, F., Kevan, P.G. and Nasr, M.E., 1995. The variability in settling velocities of some pollen and spores. Grana, 34: 39-44.

Flottum, P.K., Robacker, D.C. and Erickson, E.H.J., 1984. A quantitative sampling method for airborne sweet corn pollen under field conditions. Crop Science, 24: 375-377.

Gash, J.H.C., 1986. Observation of turbulence downwind of a forest-heath interface. Boundary-Layer Meteorology, 36: 227-237.

Gregory, P.H., 1973. Microbiology of the atmosphere. John Wiley & sons, New York, Toronto, 377 pp.

Heisler, G.M. and DeWalle, D.R., 1988. Effects of windbreak structure on wind flow. Agriculture, Ecosystems, and Environment, 18(22/23): 41-69.

Klein, E.K., 2000. Estimation de la fonction de dispersion du pollen. Application à la dissémination de trangènes dans l'environnement. Ph.D. Thesis, Paris Sud University, 80 pp.

Lacey, J. and Venette, J., 1995. Outdoor air sampling techniques. In: C.S. Cox and C.M. Wathes (Editors), Bioaerosols Handbook. Lewis, Boca Raton, FL., pp. 407-471.

Lavigne, C., Klein, E.K., Vallée, P., Pierre, J., Godelle, B. and Renard, M., 1998. A pollen dispersal experiment with transgenic oilseed rape. Estimation of the average pollen dispersal of an individual plant within a field. Theoretical and Applied Genetics, 96(6/7): 886-896.

Leuzzi, G. and Monti, P., 1998. Particle trajectory simulation of dispersion around a building. Atmospheric Environment, 32(2): 203-214.

McCartney, H.A. and Aylor, D.E., 1987. Relative contributions of sedimentation and impaction to deposition of particles in a crop canopy. Agricultural and Forest Meteorology, 40: 343-358.McCartney, H.A., Fitt, B.D.L. and Schmechel, D., 1997. Sampling bioaerosols in plant pathology. Journal of Aerosol Science, 28(3): 349-364.

McCartney, H.A. and Lacey, M.E., 1991. Wind dispersal of pollen from crops of oilseed rape (*Brassica napus* L.). Journal of Aerosol Science, 22(4): 467-477.

Panofsky, H.A. and Dutton, J.A., 1984. Atmospheric turbulence. Models and methods for engineering applications. John Wiley & sons, Inc., New York.

Raynor, G.S., Ogden, E.C. and Haynes, J.V., 1970. Dispersion and deposition of ragweed pollen from experimental sources. Journal of Applied Meteorology, 9: 885-895.

Raynor, G.S., Ogden, E.C. and Haynes, J.V., 1972a. Dispersion and deposition of corn pollen from experimental sources. Agronomy Journal, 64: 420-427.

Raynor, G.S., Ogden, E.C. and Haynes, J.V., 1972b. Dispersion and deposition of timothy pollen from experimental sources. Agricultural Meteorology, 9: 347-366.

Reynolds, A.M., 2000. Prediction of particle deposition on to rough surfaces. Agricultural and Forest Meteorology, 104: 107-118.

Scott, R.K., 1970. The effect of weather on the concentration of pollen within sugar-beet seed crops. Annals of Applied Biology, 66: 119-127.

Snyder, W.H. and Lumley, J.L., 1971. Some measurements of particle velocity autocorrelation functions in a turbulent flow. Journal of Fluid Mechanics, 48(I): 41-71.

Thomson, D.J., 1987. Criteria for the selection of stochastic models of particle trajectories in turbulent flows. Journal of Fluid Mechanics, 180: 529-556.

Wilson, J.D. and Shum, W.K.N., 1992. A re-examination of the integrated horizontal flux method for estimating volatilisation from circular plots. Agricultural and Forest Meteorology, 57: 281-295.

Wilson, J.D., 2000. Trajectory models for heavy particles in atmospheric turbulence : comparison with observations. Journal of Applied Meteorology, 39: 1894-1912.

Zhuang, Y. and Wilson, J.D., 1993. Coherent motions in windbreak flow. Boundary-Layer Meteorology, 70: 151-160.

Figure Captions

Figure 1. Experimental design. (■) sonic anemometers, (◆) the meteorological mast and Burkard trap, (▲) the mass balance masts, and (▯) the deposition plates. The mass balance masts, and deposition plates were moved so that they were downwind of the source plot. Prevailing direction of wind was generally from 225°.

Figure 2. Two-hourly moving average airborne pollen concentration above the source plot, as measured with the Burkard trap (continuous line), compared with the estimated daily pollen production (dotted line).

Figure 3. (a) Pollen concentration and surface wetness index (*SWI*) measured in the source plot between 29 July and 3 August 2000. (b) Average daily pattern of pollen concentration measured above the source plot. The concentrations were normalised with the maximum concentration of the day before taking the average. The bold line represents the mean for five days (29, 30, 31 July; 1 and 2 August), and error bars represent the standard deviation over these days. The dotted line shows the emission pattern measured on the 3 August.

Figure 4. Vertical profiles of pollen concentration measured downwind of the source plot using rotating-arm spore traps at x = 3 m (dotted line) and x = 10 m (solid line) for runs R6 (a), R7 (b) and R8 (c). Error bars were estimated as the mean standard error over the two rods of each rotating-arm.

Figure 5. Vertical profiles of wind speed normalised by the wind speed at the greatest height (4 m) and averaged over all runs at x = 3 m (black line) and x = 10 m (grey line). The log profile (dotted line) with z_0 = 0.07 m in neutral condition (u_* = 0.2 m s^{-1} and L = - ∞) is also drawn. Open circles represent values of the 12 runs 3 m downwind of the source plot and cross symbols represent values of the 12 runs 10 m downwind. Error bars show the standard deviation over the different runs.

Figure 6. Vertical profiles of horizontal flux of pollen F_x at x = 3 m (dotted line) and x = 10 m (solid line) for runs R6 (a), R7 (b) and R8 (c). Error bars were estimated as the sum of the relative errors on wind-speed and concentration.

Figure 7. Measured deposition rate divided by the measured deposition rate at x = 1 m, as a function of downwind distance from the source for runs R1 to R2 and R4 to R12. The mean deposition rate is shown as a bold line with filled circles.

Figure 8. Median normalised concentration profile, estimated over runs R1-R2, R4-R12 at x = 3 m and x = 10 m. The error bars show the standard deviation over the different runs. The profiles were normalised by dividing by the maximum concentration measured at the 3 m mast for each run, and subsequently averaged by taking the median over all runs.

Figure 9. Pollen deposition between x = 3 m and x = 10 m, estimated with the mass balance technique compared to the measured deposition rates. Open symbols show runs R3, R9, R10 and R12, where the wind direction relative to the masts was larger than 30%. A linear regression gives y = 0.98x – 16 (R^2 = 0.8).

Tables

Table 1. Location and description of the meteorological instruments used during the experiment. Height is height above ground. Negative height denotes measurements in the soil.

Parameter	Symbol	Height m	Location	Type/Source
Global radiation	R_g	5	Source plot	Pyranometer, model CM6, Kipp & Zonen, Delft, the Netherlands
Net radiation	R_n	2	Bare soil	Net radiometer, model S-1, Swissteco, Oberriet, Switzerland
Relative humidity	RH	2.1 and 4.1	Source plot	Capacitive hygrometer, Vaisala, Helsinki, Finland
Surface wetness index	SWI	2.1	Source plot	Wetness grid sensor model 237 Campbell scientific, Shepshed, UK
Air temperature	T_a	2.1 and 4.1	Source plot	0.2 mm² copper-constantan thermocouples, Thermoelectric Limeil Brévannes, France
Horizontal wind speed	U	2.4	Source plot	Cup anemometer, MCB opto electronic, Courbevoie, France
Friction velocity & Monin-Obukhov length	u_* L	1.1 2 3.95	Bare soil Source plot Target field	Ultrasonic anemometer, Model R2, Gill instruments, Lymington, UK
Wind direction	WD	5	Source plot	Wind-vane, INRA own design, France
Ground heat flux	G	- 0.1	Bare soil	Flux plates, Campbell scientific, Shepshed, UK
Horizontal wind speed	U	0.25, 0.5, 1.0, 2.0 and 4.0	Flux profile masts	Cup anemometer, MCB opto electronic, Courbevoie, France; CIMEL, Paris, France
Rainfall	Rain	1.0	Bare soil	Rain gauge, Campbell scientific, Shepshed, UK

Table 2. Date, solar time, sampling line orientation and average micrometeorological conditions measured above and within the source plot during each experimental run. R_g - global solar radiation; *RH* - relative humidity; *SWI* – surface wetness index; *rain* – rainfall; T_a - air temperature; *VPD* - vapour pressure deficit of the air; *U* - wind speed, *WD* - wind direction and *WDr* – wind direction relative to sampling line direction. All measurements were made at a height of 2.1 m except *U* which was measured at 2.4 m and R_g and *WD* which were measured at 5 m. u_*, the friction velocity, and *L*, the Monin-Obukhov length, were measured with the sonic anemometers. Means and standard deviation are given.

		Experiment		R_g	*RH*	*SWI*	*rain*	T_a	*VPD*	*U*	u_*	*L*	*WD*	*WDr*
Run	**Date**	**Time (UT*)**	**Sampling line direction (deg)**	**W m^{-2}**	**%**	**%**	**mm**	**°C**	**kPa**	**m s^{-1}**	**m s^{-1}**	**m**	**deg**	**deg / sampling line direction**
R1	25 July	0830-1030	248	595 ± 145	81 ± 5	0	0	19.4 ± 0.8	0.44 ± 0.14	0.8 ± 0.1	0.21 ± 0.05	-10	256 ± 18	8
R2	25 July	1100-1400	250	680 ± 168	61 ± 3	0	0	23.3 ± 0.6	1.13 ± 0.13	0.6 ± 0.1	0.17 ± 0.05	-6	241 ± 27	-9
R3	25 July	1430-1530	250	98 ± 77	70 ± 11	50	0	21.2 ± 1.5	0.78 ± 0.34	0.4 ± 0.2	0.08 ± 0.01	-4	209 ± 52	-41
R4	26 July	0800-1000	250	468 ± 106	80 ± 4	0	0	19.8 ± 0.8	0.45 ± 0.11	0.9 ± 0.2	0.25 ± 0.08	-22	247 ± 20	-3
R5	26 July	1315-1515	250	679 ± 135	57 ± 2	0	0	24.8 ± 0.4	1.35 ± 0.09	0.7 ± 0.1	0.31 ± 0.05	-48	244 ± 10	-6
R6	27 July	0800-1000	250	242 ± 96	81 ± 2	1	0	19.1 ± 0.4	0.43 ± 0.05	0.7 ± 0.1	0.21 ± 0.05	-36	233 ± 17	-17
R7	27 July	1245-1415	250	298 ± 94	69 ± 2	2	0	21.1 ± 0.4	0.76 ± 0.08	0.6 ± 0.1	0.17 ± 0.07	-14	266 ± 8	16
R8	28 July	0745-0815	270	352 ± 183	83 ± 1	4	1.6	18.7 ± 0.8	0.36 ± 0.10	0.9 ± 0.1	0.26 ± 0.1	-43	263 ± 5	-7
R9	30 July	0815-1015	270	700 ± 151	63 ± 4	0	0	22.6 ± 1.1	1.02 ± 0.18	0.1 ± 0.1	0.12 ± 0.09	-**	153 ± 42	-117
R10	30 July	1300-1500	270	690 ± 201	52 ± 3	0	0	24.7 ± 0.8	1.51 ± 0.13	0.6 ± 0.1	0.19 ± 0.09	-16	302 ± 19	32
R11	31 July	0730-0930	117	583 ± 79	64 ± 9	12	0	23.2 ± 1.9	1.06 ± 0.36	0.4 ± 0.1	0.13 ± 0.11	-9	98 ± 15	-19
R12	31 July	1000-1230	117	751 ± 98	50 ± 2	0	0	26.3 ± 0.7	1.73 ± 0.11	0.4 ± 0.1	0.17 ± 0.004	-8	154 ± 22	37

* Universal Time (roughly close to solar time. In France, it is local time –0200 in summer)

** Monin-Obukhov length was out of its range of validity, and as u_* was small this suggests that the conditions during this run were close to free convection.

Table 3. Number of plants starting and ending flowering, and daily pollen production per plant. The flowering status was estimated by observing 25 plants, pollen production was assessed from the same 5 individual plants. The total production over the pollination period was 1.4×10^7 grains plant^{-1}.

Day of year 2000	**Plants starting flowering**	**Plants ending flowering**	**Daily pollen production for the whole field**	
	%	%	grains day^{-1} plant^{-1}	% of the total pollen production
25/07	0	0	1.3×10^4	0.1
26/07	4	0	1.9×10^5	1.3
27/07	16	0	3.3×10^5	2.4
28/07	12	0	5.5×10^5	4.0
29/07	16	0	1.0×10^6	7.4
30/07	20	0	1.3×10^6	9.2
31/07	20	0	1.7×10^6	12.2
01/08	8	0	1.9×10^6	13.5
02/08	0	20	1.8×10^6	13.0
03/08	4	8	1.7×10^6	12.3
04/08	0	4	1.3×10^6	9.6
05/08	0	28	9.7×10^5	7.0
06/08	0	12	5.8×10^5	4.2
07/08	0	16	2.9×10^5	2.1
08/08	0	8	1.3×10^5	1.0
09/08	0	4	5.0×10^4	0.4
10/08	0	0	1.8×10^4	0.1

Table 4. Pollen production, integrated deposition rates and horizontal fluxes at different distances downwind of the source. The measured deposition rate at x = 1 m is also given as a reference for Figure 7. $D_{1\text{-}3}$ is the integrated deposition rate between x = 1 and 3 m, $D_{1\text{-}32}$ is the integrated deposition rate between x = 1 and 32, $D_{3\text{-}10}$ is the integrated deposition rate between x = 3 and 10 m, downwind of the source. Also shown are estimates of the horizontal flux, integrated between z = 0 and z = 4 m height, at x = 3 m ($F_3^{\{0\text{-}4\}}$) and x = 10 m ($F_{10}^{\{0\text{-}4\}}$) downwind of the source. $\Delta F_{3\text{-}10}$ is the horizontal flux difference between x = 3 and x = 10 m. The integrated deposition rates $D_{1\text{-}3}$ and $D_{1\text{-}32}$ are also expressed in percentage of the pollen production per meter of lateral width of the source. Runs lasted between 90 and 180 min. - denotes lack of data.

	Pollen production	Deposition rate at x = 1 m	Deposition rate integrated over x					Horizontal flux		
Run			$D_{1\text{-}3}$		$D_{1\text{-}32}$		$D_{3\text{-}10}$	$F_3^{\{0\text{-}4\}}$	$F_{10}^{\{0\text{-}4\}}$	$\Delta F_{3\text{-}10}$
	grains m^{-1} s^{-1}	grains m^{-2} s^{-1}	grains m^{-1} s^{-1}	%	grains m^{-1} s^{-1}	%	grains m^{-1} s^{-1}	grains m^{-1} s^{-1}	grains m^{-1} s^{-1}	grains m^{-1} s^{-1}
R1	40	14	33	81	186	462	43	34	4	30
R2	42	3	11	26	107	256	24	15	7	8
R3	12	-	-	-	-	-	-	1	0	1
R4	862	23	94	11	505	59	189	276	22	254
R5	478	14	42	9	-	30	69	80	66	15
R6	763	69	201	26	449	59	158	370	172	197
R7	935	50	110	12	339	36	84	89	34	55
R8	3068	45	198	6	812	26	308	556	248	308
R9	14679	141	322	2	918	6	277	208	62	146
R10	2043	8	53	3	258	13	84	101	51	50
R11	3551	138	331	9	865	24	249	293	66	227
R12	16833	138	415	2	1183	7	387	434	115	319

Figures

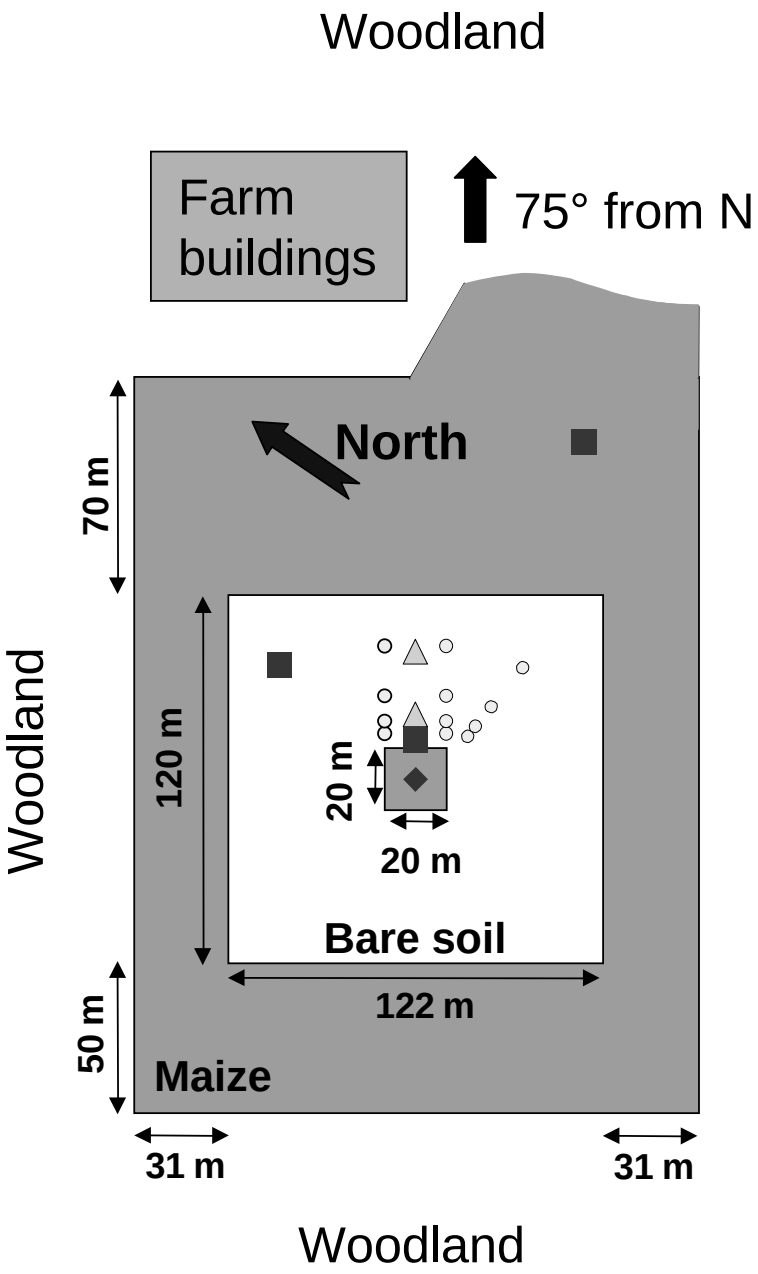

FIGURE 1

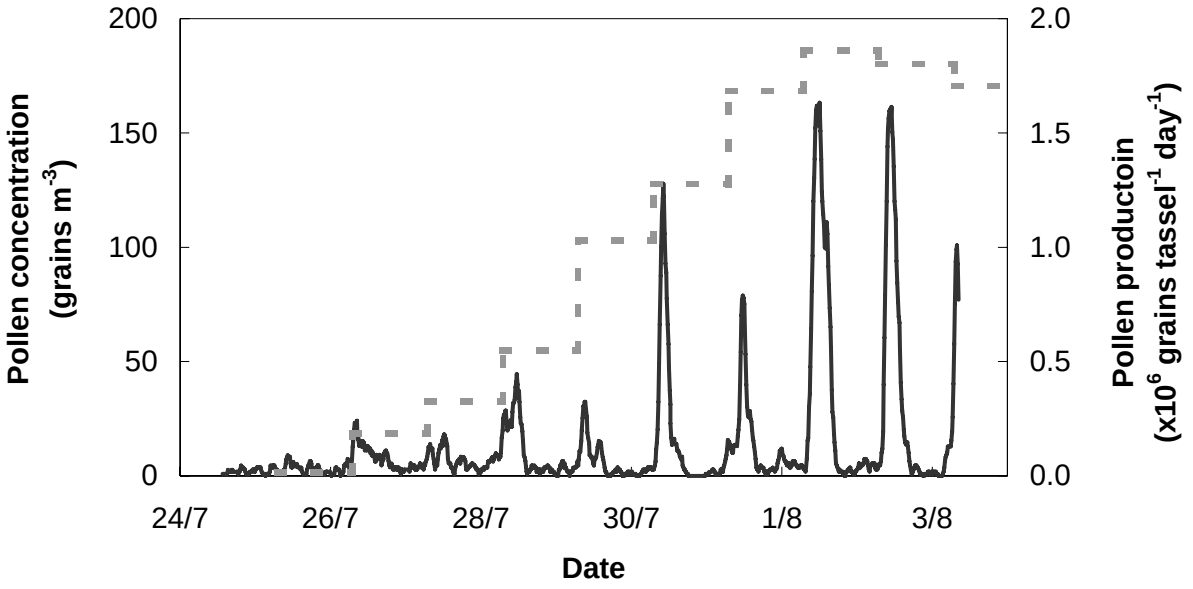
200
150
100
50
0
2.0
1.5
1.0
0.5
0.0
Pollen concentration (grains m-3)
Pollen productoin (x10^6 grains tassel-1 day-1)
24/7
26/7
28/7
30/7
1/8
3/8
Date

FIGURE 2

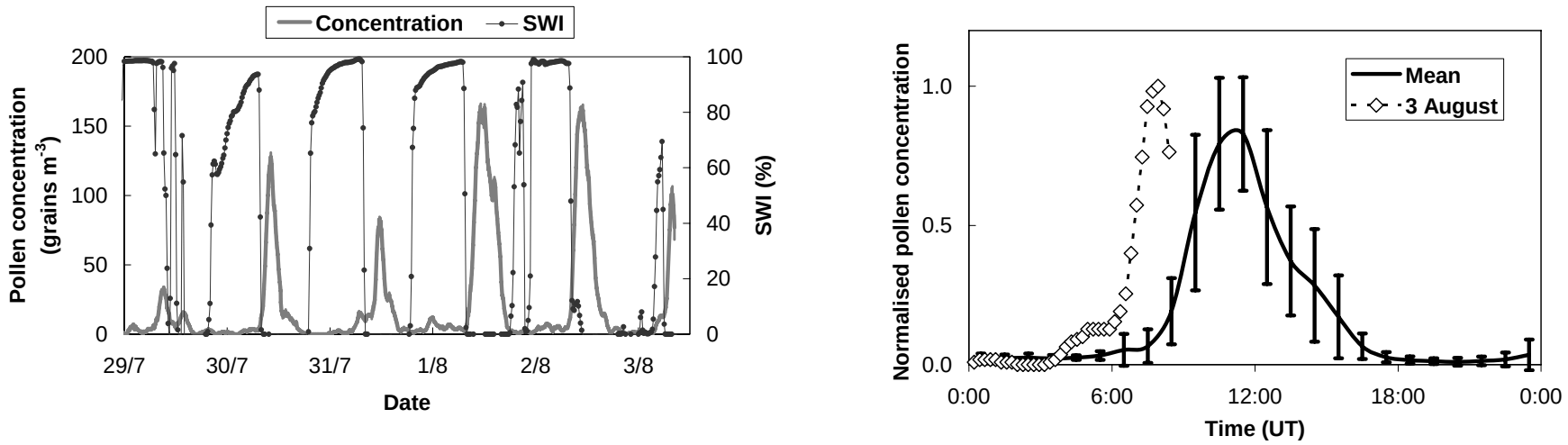
(a)
(b)
Concentration
SWI
Pollen concentration (grains m-3)
SWI (%)
Date
29/7
30/7
31/7
1/8
2/8
3/8
Normalised pollen concentration
Mean
3 August
Time (UT)
0:00
6:00
12:00
18:00
0:00

FIGURE 3

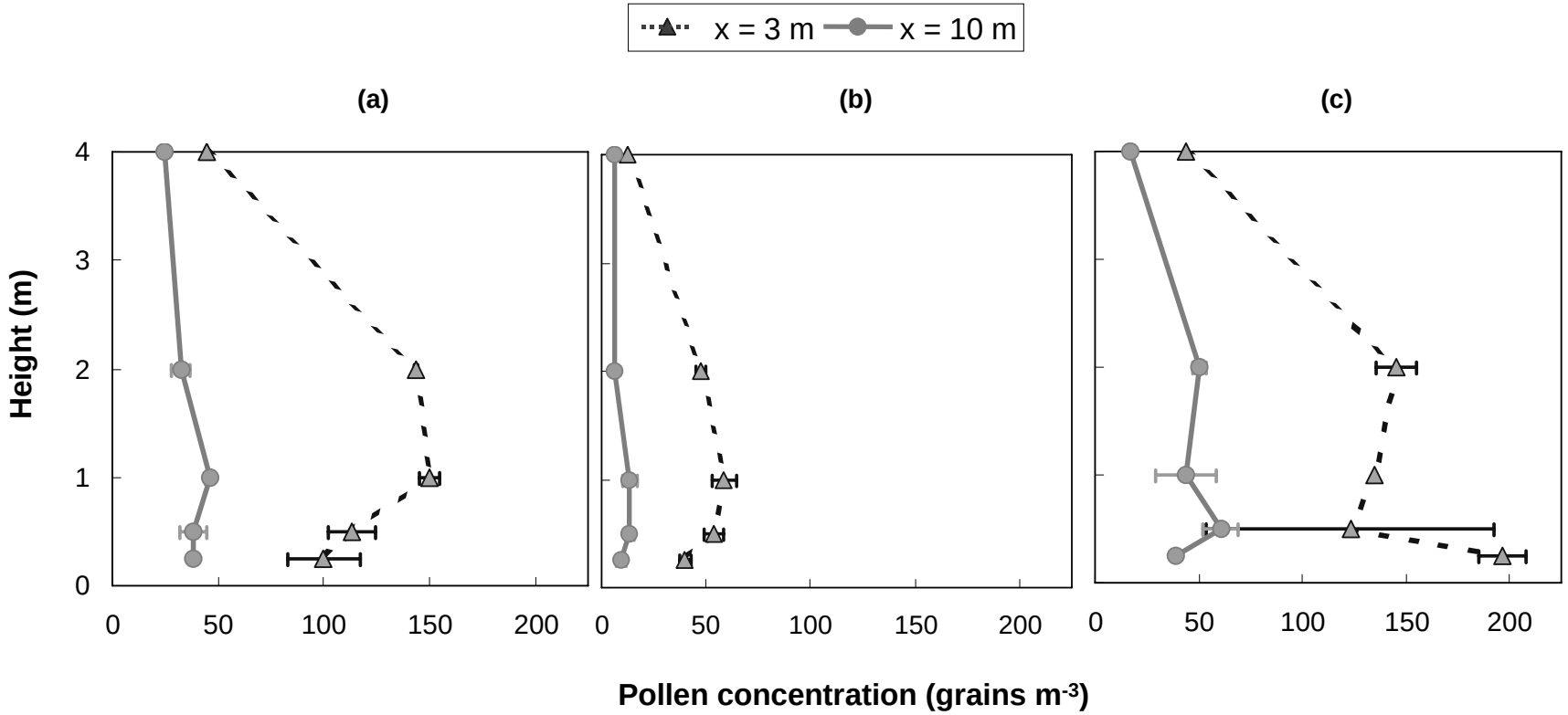
x = 3 m
x = 10 m
(a)
(b)
(c)
Height (m)
0
1
2
3
4
0
50
100
150
200
Pollen concentration (grains m-3)

FIGURE 4

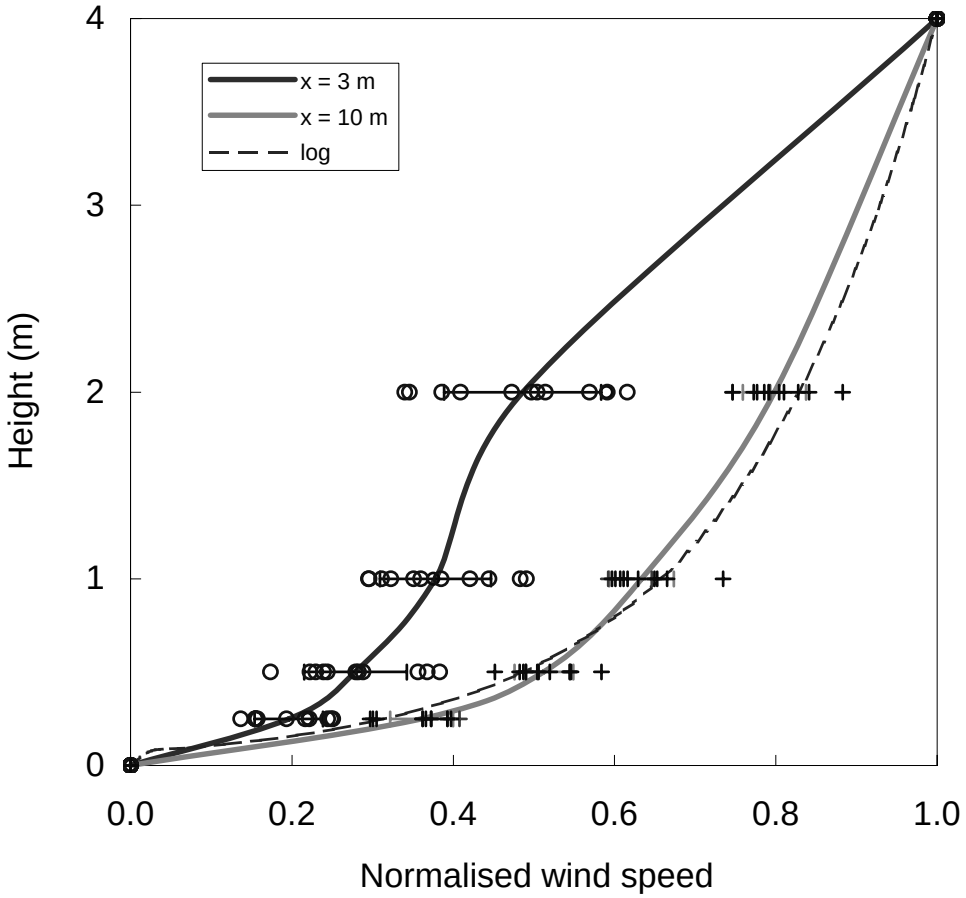
x = 3 m
x = 10 m
log
Height (m)
Normalised wind speed
0
1
2
3
4
0.0
0.2
0.4
0.6
0.8
1.0

FIGURE 5

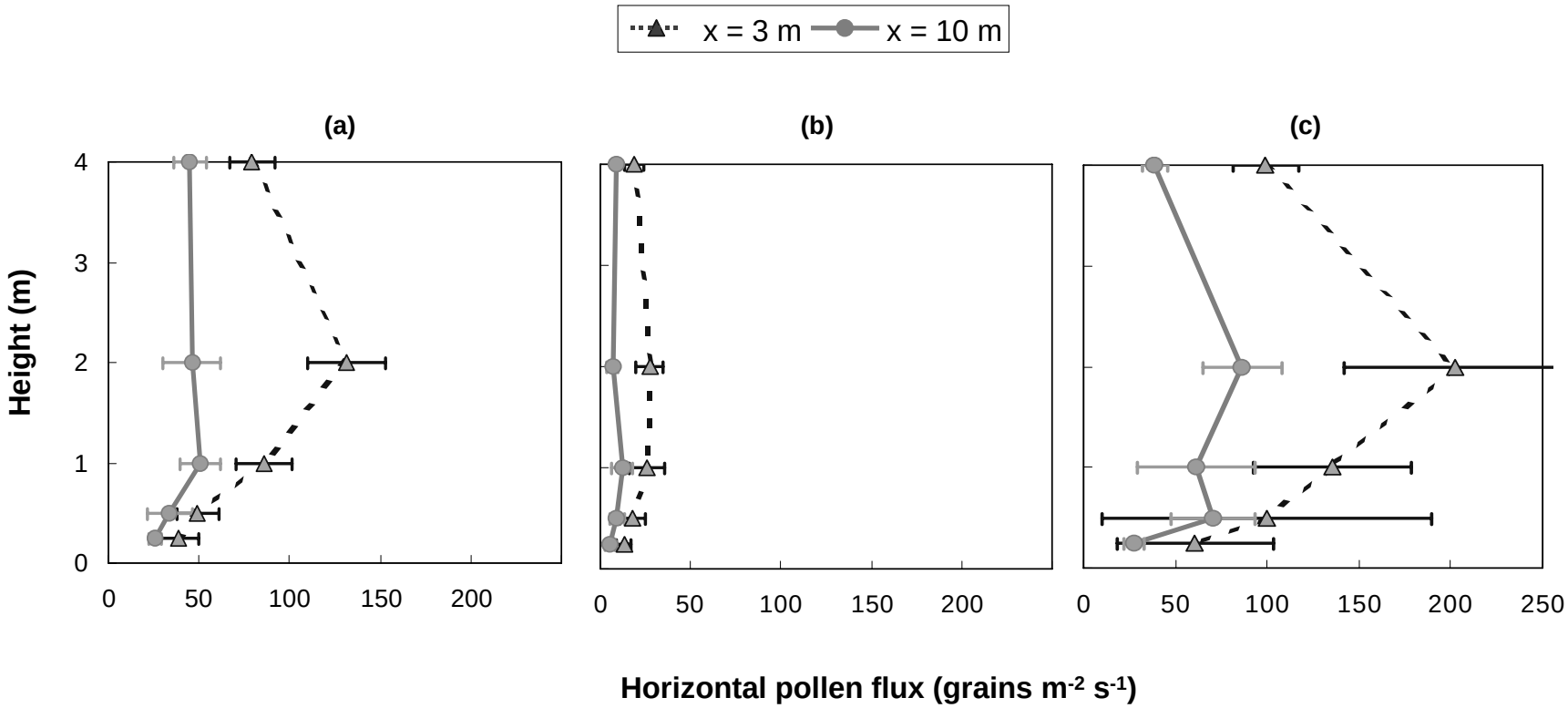
x = 3 m
x = 10 m
(a)
(b)
(c)
Height (m)
0
1
2
3
4
0
50
100
150
200
250
Horizontal pollen flux (grains m-2 s-1)

FIGURE 6

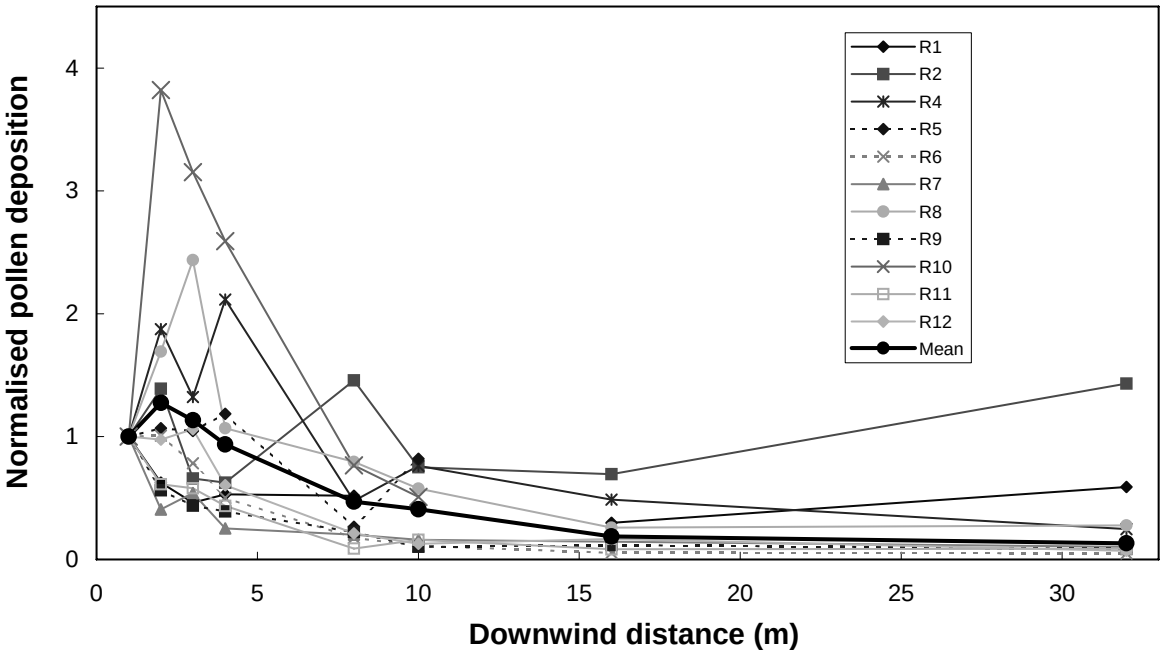
Normalised pollen deposition
Downwind distance (m)
0
1
2
3
4
0
5
10
15
20
25
30
R1
R2
R4
R5
R6
R7
R8
R9
R10
R11
R12
Mean

FIGURE 7

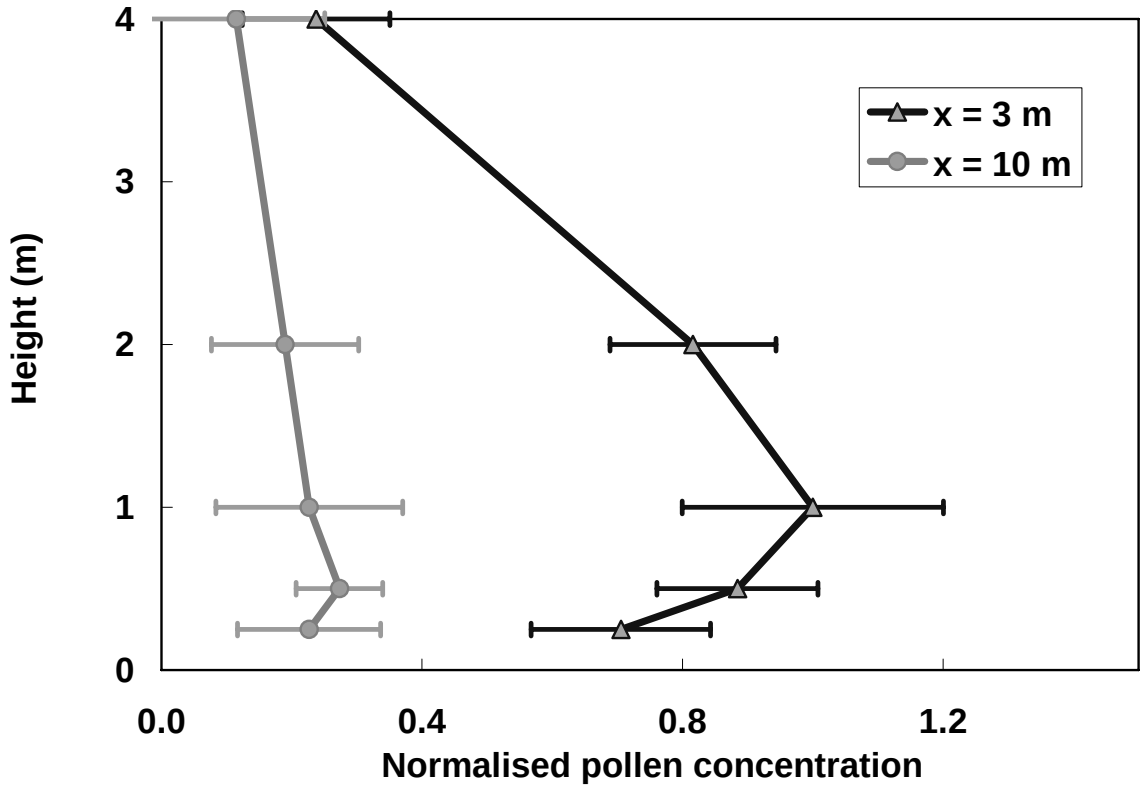
4
3
2
1
0
Height (m)
0.0
0.4
0.8
1.2
Normalised pollen concentration
x = 3 m
x = 10 m

FIGURE 8

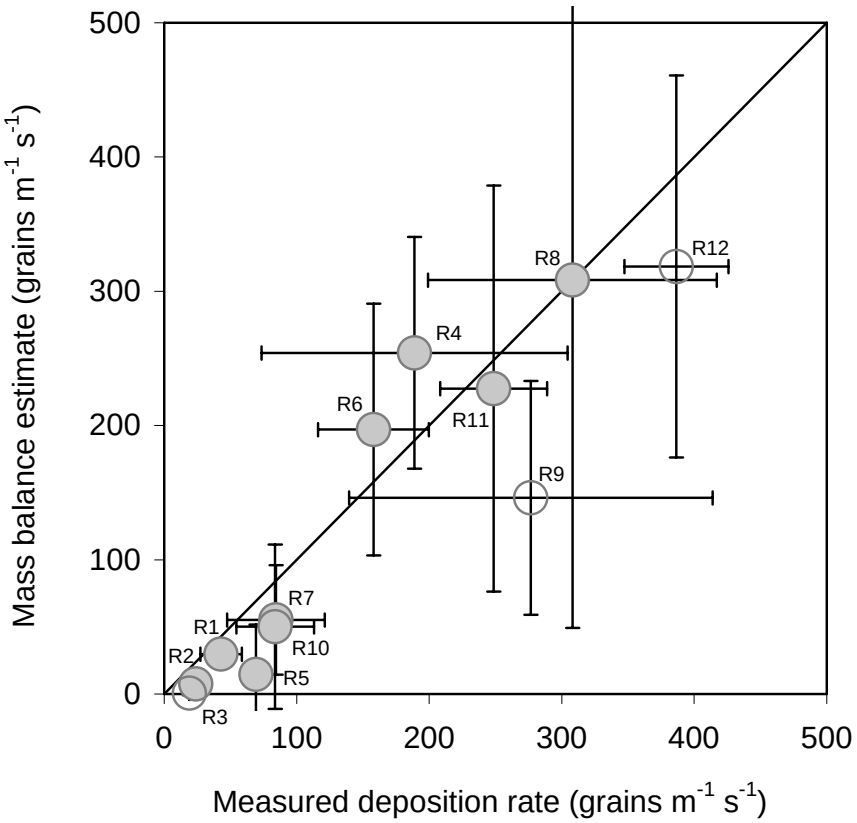
Mass balance estimate (grains m-1 s-1)
Measured deposition rate (grains m-1 s-1)
0
100
200
300
400
500
R1
R2
R3
R4
R5
R6
R7
R8
R9
R10
R11
R12

FIGURE 9